


1 **Independent Comparative Evaluation of the Pupil Neon - A New Mobile**
2 **Eye-tracker**

3 Valentin Foucher¹, Alina Krug¹, and Marian Sauter¹

4 ¹Ulm University, Insitute of Psychology, General Psychology

5 **Author Note**

6 August 7, 2024: Stage 1 Submission for Peer Community in Registered Reports

7 Valentin Foucher  <https://orcid.org/0009-0000-2632-3519>

8 Alina Krug  <https://orcid.org/0009-0004-7088-1584>

9 Marian Sauter  <https://orcid.org/0000-0003-3123-8073>

Abstract

10

11 [testtestest](#)Due to the rapid adoption of (mobile) eye-tracking devices in both academic
12 and consumer research, it becomes more important that the increasing number of datasets
13 is based on reliable recordings. This study provides an independent evaluation of the Pupil
14 Neon (Pupil Labs GmbH), one of the newest and most affordable mobile eye-trackers, by
15 comparing its performance on a variety of tasks to the EyeLink 1000 Plus (SR Research
16 Ltd.). Using Ehinger et al. (2019)'s test battery, a set of 10 tasks evaluated the accuracy
17 and its decay over time of some of the most common eye-tracking-related parameters:
18 fixations, saccades, smooth pursuit, pupil dilation, microsaccades, blinks, and the influence
19 of head motion on accuracy. Gaze position, eye movements and pupil diameter associated
20 with each task were recorded simultaneously by the two eye-trackers and compared
21 concurrently. The results provide some ideas on what singularities should be expected by
22 the newer Pupil Neon for the recording of specific eye movements or the performance in
23 various kinds of tasks.

24

Keywords: eye tracking, mobile eye-tracker, Pupil Neon, Eyelink 1000 Plus,

25

performance evaluation

Independent Comparative Evaluation of the Pupil Neon - A New Mobile Eye-tracker

Introduction

The saying "One look is worth a thousand words" highlights the significant role of eye movements in understanding how individuals perceive and interpret their world. This concept has been extensively applied in fields such as psychology and human-computer interaction (Duchowski, 2007; Majaranta & Bulling, 2014). Over the past decades, eye-trackers, once confined to a small group of researchers, have become widely available to a broader audience (Duchowski, 2018; Gunawardena et al., 2022), including applied researchers (Ahlström et al., 2021) and practitioners in marketing and gaming (Mancini et al., 2022). The increase in reliability, coupled with less invasive devices and more affordable prices, has democratized the use of eye-trackers to study human behavior. However, the expanding range of eye-tracking applications makes it crucial to understand the performance of current eye-trackers and how their capabilities and limitations make them suitable for different types of experimental protocols (Titz et al., 2018). This study aims to evaluate the performance of a recently released mobile eye-tracker, the Pupil Neon from Pupil Labs, by examining some of the most common eye-tracking-related parameters: fixations, saccades, smooth pursuit, pupil dilation, microsaccades, blinks, and the influence of head motion on accuracy (Duchowski, 2018). By conducting this independent comparative evaluation, we seek to provide researchers with information on the strengths and weaknesses of the Pupil Neon, facilitating its effective use in diverse research contexts.

Stationary and mobile eye-trackers

Two types of eye-tracking devices are usually distinguished: stationary (or desk/screen-mounted) eye-trackers, and mobile (or head-mounted) eye-trackers (Pentus et al., 2020).

Stationary eye-trackers are ideal for two-dimensional stimuli presented via screen-based tasks, making them traditionally popular in basic research where a controlled

53 experimental setup is feasible (Holmqvist et al., 2011). These eye-trackers often have high
54 accuracy and precision, potentially reaching up to 0.3 degrees under optimal conditions
55 (Ehinger et al., 2019). However, achieving such performance comes at the cost of
56 restricting participants in their head and body movements, lowering ecological validity
57 (Holmqvist et al., 2011). Such setups often require a fixed sitting position or even head
58 fixation via chinrest, limiting natural behaviour. Additionally, the highly controlled
59 environment of lab experiments may not accurately represent real-life conditions,
60 prompting the eye-tracking scientific community to seek tools that enable monitoring in
61 real-world settings (Gunawardena et al., 2022; Takahashi et al., 2018).

62 Conversely, mobile head-mounted eye-trackers allow much more freedom in head
63 and body movements by tracking directly from sensors located on the participant's head
64 (e.g. glasses), making them a prior candidate for in-the-wild studies and applied research
65 where it is necessary to move in an environment (Bulling & Gellersen, 2010). Notably, this
66 refers to the contemporary mobile eye-trackers and not the first scleral coil eye-tracking
67 devices that were directly mounted to the participant's eye (Huey, 1900). However, this
68 freedom introduces challenges in tracking gaze accurately, resulting in noisier data and
69 lower precision, typically around 0.9 to 1.8 degrees of visual angle (Baumann & Dierkes,
70 2023; MacInnes et al., 2018). Mobile eye-trackers also face technical issues such as device
71 heating, which can affect user experience, limited battery life leading to restricted data
72 collection duration, and the need for a stable wireless connection (Gunawardena et al.,
73 2022). Despite these challenges, technological advancements are continuously improving
74 the performance of mobile eye-trackers, necessitating regular updates on their capabilities.
75 In the present study, we aim to assess the performance of one of the most recent mobile
76 eye-tracking devices on the market.

77 **Evaluating eye-tracker performances**

78 Evaluating the performances of data recording devices is essential for any research
79 field, as it allows the assessment of data quality and reliability. Understanding the

80 capabilities and limitations of eye-trackers is essential in order to optimizing their
81 utilization. While several studies have examined data quality from field eye-tracking
82 experiments in various experimental contexts (Funke et al., 2016; Hooge et al., 2023;
83 MacInnes et al., 2018; Niehorster et al., 2020) or using artificial eyes (Wang et al., 2017),
84 the complexity and diversity of human eye movements should also be considered when
85 measuring an eye-tracker's performances (Holmqvist et al., 2012). Estimating an
86 eye-tracker's performance is challenging, as comparisons to a theoretical true value are not
87 possible (Ehinger et al., 2019). When asking participants to fixate on a visual stimulus for
88 calibration, the actual eye fixation point is not steady due to miniature, unconscious eye
89 movements like drift and microsaccades, which can corrupt the recorded fixation baseline
90 (Rolfs, 2009). To address this lack of a truth reference, earlier studies used two eye-trackers
91 simultaneously to evaluate and compare their performances across a variety of tasks
92 (Drewes et al., 2011; Ehinger et al., 2019; Titz et al., 2018): a reference and a target
93 eye-tracker to be evaluated. Building on the study conducted by Ehinger et al. (2019), the
94 current study uses the Eyelink 1000 (SR Research Ltd., 2022) as a reference eye-tracker
95 due to its high precision and accuracy. It is considered one of the best video-based
96 eye-trackers available (Holmqvist, 2017; Kaduk et al., 2023). Comparing a mobile
97 eye-tracker to a stationary one in terms of gaze accuracy and precision may appear to be of
98 limited value, given that these two types of eye-trackers often serve different purposes. The
99 goal of such comparisons is not to favour one type of device over another, but rather to
100 highlight the distinctive characteristics exhibited by each device when recording specific
101 types of eye movements. Various types of eye movements, including changes in pupil size
102 provide diverse information about visual and cognitive processing (Martinez-Conde et al.,
103 2004; Rayner, 2009; Rayner, 1998). For example, fixations are essential for detailed visual
104 processing and information acquisition, allowing the eyes to remain steady and to absorb
105 information from a specific area of the visual field (Henderson, 2003). Saccades are rapid
106 eye movements that reposition the fovea to a new location of interest and are critical for

107 visual attention and scene perception (Rayner, 1998). Microsaccades however are tiny,
108 involuntary eye movements that help in the fine-tuning of visual fixation and are linked to
109 covert attention (Martinez-Conde et al., 2004; Martinez-Conde et al., 2013). Relative to
110 saccades, smooth pursuits are characterized by slow eye movements to maintain a moving
111 object on the fovea and are associated with tracking moving stimuli (Krauzlis, 2004). Eye
112 blinks can indicate cognitive load and fatigue (Schleicher et al., 2008) and changes in pupil
113 size are indicative of arousal and cognitive effort (Beatty & Lucero-Wagoner, 2000). Each
114 type of eye-based measure has specific tracking requirements: the accuracy of fixations and
115 saccades is impaired by head movements, particularly in free-viewing or or extreme head
116 movement conditions (Einhäuser et al., 2007). Pupillometry also demands minimal head
117 movement, a fixed stimulus position and steady brightness conditions (Mathôt &
118 Vilotijević, 2023). The analysis of smooth pursuits however requires smooth stimuli
119 velocity and a high temporal resolution to distinguish from saccades and microsaccades
120 (Holmqvist et al., 2011); blink frequency is influenced by fatigue and experiment duration
121 (Schleicher et al., 2008). To adequately evaluate an eye-tracker’s performance, it is essential
122 to consider more than just the accuracy and precision typically reported by manufacturers.
123 To date, publicly available data are limited, and independent evaluations are even scarcer.
124 To address this, Ehinger et al. (2019) developed a comprehensive evaluation paradigm,
125 assessing fixation and saccade accuracy in grid and free-viewing tasks, accuracy decay over
126 time, smooth pursuit, pupil dilation, microsaccades, blinks, and the influence of head
127 motion. At the time of their evaluation, mobile eye-trackers such as the Pupil Core (Pupil
128 Labs GmbH) predominantly recorded the eyes with infrared video-based methods and
129 detected the pupil using common computer vision algorithms to track gaze. Instead of
130 ‘simple’ computer vision approaches based on infrared eye-tracking, the newer Pupil Neon
131 (Pupil Labs GmbH) uses a proprietary deep learning approach. It has the advantage that
132 it is supposedly more flexible in terms of environmental context and does not require a
133 calibration procedure. However, it has the disadvantage inherent to all deep learning

134 approaches: we do not really know how it works and thus do not know whether it captures
135 all types of eye movements equally well. Thus, this independent evaluation will benefit
136 researchers intending to use the Pupil Neon by demonstrating the advantages and
137 limitations of such eye-tracking technology before employing it in their studies.

138 **Our study**

139 Due to the rapidly increasing use of (mobile) eye-tracking devices in both academic
140 and consumer research, it becomes more important that the increasing number of datasets
141 is based on reliable recordings. Given the use case for mobile eye-tracking devices in
142 certain research and consumer settings, a major factor influencing widespread adoption is a
143 device's ease of use (Davis et al., 1989). This is our reason for choosing to evaluate the
144 Pupil Neon over other mobile eye-tracking devices. To our knowledge, it is the only device
145 that requires no calibration, significantly simplifying setup and reducing the time required
146 for participants to begin tasks. Moreover, the Pupil Neon is one of the more affordable
147 options available, with costs starting at €5,950 as of July 2024, making it accessible to a
148 broader range of researchers and institutions. Recent manufacturer evaluations indicate
149 that despite not having a calibration procedure, it performs comparably well with an
150 accuracy of around 1.3° (Baumann & Dierkes, 2023). However, it employs a proprietary
151 deep-learning algorithm for calibration-free classification of eye movements, which
152 complicates performance evaluation based solely on available data and code. This study
153 aims to provide an independent evaluation of the Pupil Neon's performance across various
154 eye-based tasks. Following Ehinger et al. (2019) procedure, participants will perform a set
155 of tasks while being tracked simultaneously by both the Pupil Neon and the EyeLink 1000.
156 These tasks include fixations on a large grid to assess spatial accuracy, smooth pursuit
157 tasks, free viewing tasks to evaluate eye movements and gaze trajectories, microsaccades
158 tasks, blink tasks, pupil dilation tasks, fixations on a small grid to evaluate the decay of
159 accuracy over time, head yaw movements, head roll movements, and fixations on a small
160 grid after head movements to assess the decay of accuracy. The results will provide insights

161 into the specific characteristics and performance of the Pupil Neon in recording various eye
162 movements and performing different tasks. These findings will help identify tasks where
163 the Pupil Neon excels and highlight tasks that might be less advisable to conduct with this
164 device due to differing eye movement requirements.

165 **Methods**

166 The methodology employed in this study is largely consistent with that described by
167 Ehinger et al. (2019).

168 **Participants**

169 We recruited *[tbd]* participants from Ulm University, with an average age of *[tbd]*
170 years (range *[tbd]* - *[tbd]* years); *[tbd]* were female, *[tbd]* were left-handed, and *[tbd]* had a
171 left-dominant eye. The inclusion criteria were: no use of glasses or **hard contact lenses**, no
172 drug use, no history of photosensitive migraines or epilepsy, and at least 5 hours of sleep
173 the night before the experiment. Written consent was obtained from all participants, and
174 the study was declared exempt from ethical approval by the ethics committee of Ulm
175 University (letter from 06.06.2024). Participants received compensation of either €12 or
176 one course-credit per hour. *[tbd]* participants were excluded from the analysis since they
177 exceeded the predetermined calibration accuracy limits of the EyeLink 1000.

178 **Experimental setup and recording devices**

179 The experimental setup and recording devices are largely similar to those employed
180 by Ehinger et al. (2019), except for the use of the Pupil Neon glasses instead of the Pupil
181 Core glasses. The description of the experimental setup and recording devices is adapted
182 from Ehinger et al. (2019). The experiment took place in a light and soundproof laboratory
183 at Ulm University. The lights were left on during the experimental procedure to ensure
184 constant lighting conditions throughout the experiment. The original experimental code
185 was written by Ehinger et al. (2019) in MATLAB (2016). In the present study, the code
186 was adapted and programmed in MATLAB (2021) on a computer with Windows 10 OS
187 using the Psychophysics Toolbox 3 (Brainard & Vision, 1997; Kleiner et al., 2007; Pelli,

1997), EyeLink Toolbox (Cornelissen et al., 2002), and custom scripts based on the ZMQ
protocol for communication with the Pupil Neon. Stimuli were presented on an ASUS
ROG SWIFT PG279QM screen (27 inch, 2560 × 1440 pix) running at 100 Hz. Stimuli
were presented on a constant gray background, except for the pupil dilation task, in which
different backgrounds were used to stimulate pupil dilation and constriction. The
participants were seated at a distance of 60 cm from the screen, at which the display
subtends $[tbd]^\circ$ x $[tbd]^\circ$ of visual angle. Two Logitech Multimedia Speakers Z200 emitted a
300 Hz sound for the auditory stimuli.

Participants' eye movements were simultaneously recorded using one stationary and
one mobile eye-tracking device. The desktop-mounted EyeLink 1000 Plus (SR Research
Ltd.) recorded monocular movements of the dominant eye at 1000 Hz in head-free mode
(Ehinger et al., 2019, cf.). Concurrently, the Pupil Labs Neon glasses (Pupil Labs GmbH.)
recorded binocular eye movements. The Pupil Labs Neon glasses include a scene camera
(1600 × 1200 pixels at 30 Hz, 132° horizontal and 81° vertical field of view) and two
infrared eye cameras (192 × 192 pixels at 200 Hz). These glasses feature real-time neural
network technology, providing binocular eye tracking without the need for calibration, and
employ deep learning for slippage compensation. Data were captured using the Neon
Companion device and pre-processed post-hoc via Pupil Cloud (see Data Analysis section).
The glasses also include an inertial measurement unit (IMU) comprising an accelerometer,
magnetometer, and gyroscope, along with dual microphones. The experiment used two
computers in addition to the Companion device: one for stimuli presentation and one for
recording the EyeLink 1000. Experimental messages ("triggers") were sent to the EyeLink
1000 recording computer via the EyeLink Toolbox (Cornelissen et al., 2002), and to the
Pupil Labs glasses using zeroMQ packages ("ZeroMQ," 2024). To synchronize the
recordings, concurrent trigger signals were sent via Ethernet during experimental events.

213 **Experimental Procedure**

214 The experimental procedure is similar to the one described by Ehinger et al. (2019),
215 from which this subsection is adapted.

216 Each session began with a brief oral instruction on the experimental procedure and
217 tasks. Then, participants' visual acuity was checked using a calibrated online LogMar chart
218 test with a single test line of five letters. A correct identification of 6/6 was required to
219 proceed with the experiment. Afterwards, Ocular dominance was determined using the
220 "hole-in-card" test with participants' hands and a centered gaze.

221 The experiment comprised six blocks, each consisting of 10 tasks (see Figure 1),
222 presented in a fixed sequence. Eye-tracker calibration was performed at the beginning of
223 each block. Afterwards, participants completed a grid task (large grid) designed to assess
224 the spatial accuracy of the eye-trackers. Afterwards, participants performed several tasks
225 without head movements comprising smooth pursuit, free viewing, microsaccades, blinks
226 and pupil dilation. Afterwards, the small grid task was performed. Then, participants
227 performed two tasks requiring head movements, namely head yaw and head roll. Half of
228 the participants started with the head yaw task, the other half with the head roll. Task
229 order was balanced between participants. At the end of each block, the small grid task was
230 performed again. Hence, tasks requiring intense fixation (microsaccade and pupil dilation)
231 were interspersed with more relaxing tasks (blinks and free viewing accuracy) to provide
232 participants with periodic breaks. Participants read written instructions prior to each task
233 and saw a green fixation target at the center of the monitor. Further, the experimenter
234 stressed the importance of focusing on the fixation targets before starting the task.
235 Participants initiated each task at their own pace by pressing the space bar. The
236 experimental session lasted approximately *[tbd]* minutes.

237 **Tasks**

238 We used the tasks and code implementation developed by Ehinger et al. (2019),
239 from which the task descriptions are adapted.

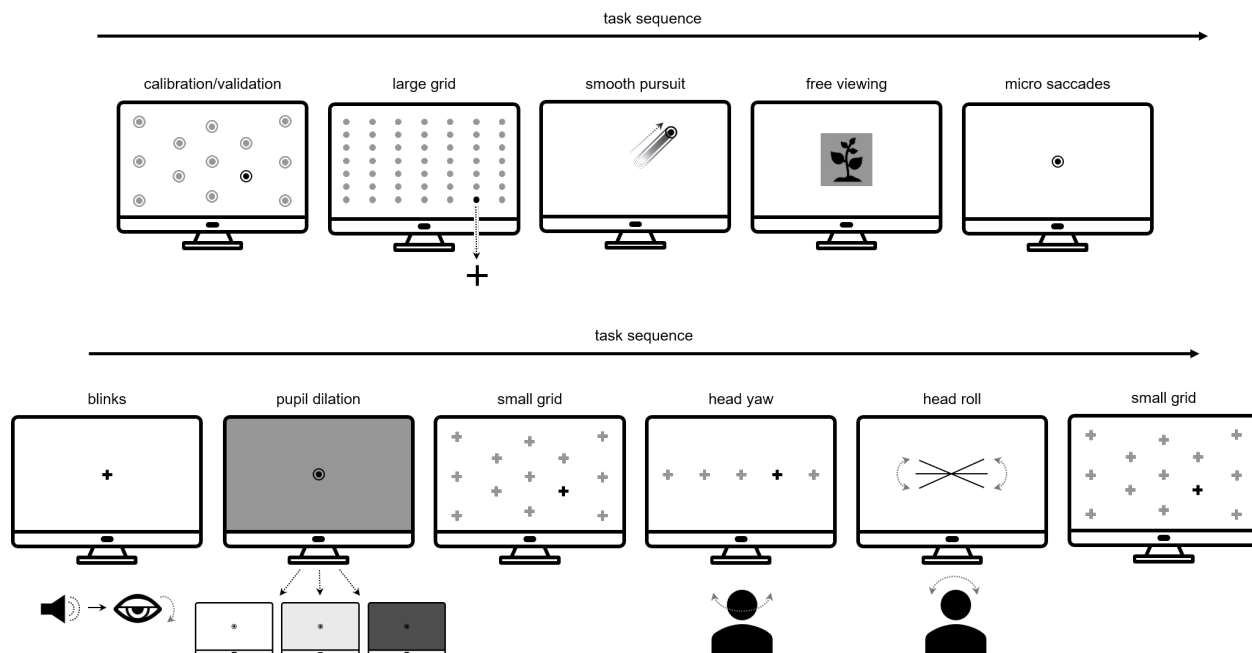


Figure 1

This figure illustrates the task sequence within each experimental block. All possible stimuli positions are marked in gray, gray dotted arrows indicate stimulus movement. Gray markings were not shown throughout the trial. For the large grid task, fixation crosses served as stimulus material. Adapted from “A new comprehensive eye-tracking test battery concurrently evaluating the Pupil Labs glasses and the EyeLink 1000” by B. V. Ehinger, K. Groß, I. Ibs, & P. König, 2019, PeerJ, 7:e7086 (<https://doi.org/10.7717/peerj.7086>).

240 Fixation targets

241 Throughout the experiment, we used three different fixation targets. For the
 242 EyeLink calibration we used the manufacturers calibration targets. For the large and small
 243 grid task, blink task, head yaw task, and head roll task a fixation cross was utilized, as it
 244 has been shown to reduce miniature eye movements (Thaler et al., 2013). For the smooth
 245 pursuit task, microsaccade task and pupil dilation task, we used a bullseye target (outer
 246 circle: black, diameter 0.5° ; inner circle: white, diameter 0.25°). For the smooth pursuit
 247 task, the bullseye was used due to its aesthetically pleasing diagonal movement. For the
 248 microsaccade task, the bullseye was used since minimization of microsaccades was not

249 desired. For the pupil dilation task, the bullseye was used due to its visibility regardless of
250 background illumination.

251 **Eye-tracker calibration**

252 The EyeLink 1000 was calibrated using a 13-point randomized calibration
253 procedure. These 13 calibration points were selected from the large grid used in the
254 accuracy task (see section “Task 1/Task 7/Task 10: Accuracy Task with the Large and the
255 Small Grid”). Calibration points were manually advanced by the experimenter. Following
256 calibration, a 13-point verification process was conducted. The procedure was identical to
257 the initial calibration, yet calibration points were presented within a new randomized
258 sequence. Accuracies were calculated online, and recalibration was performed if necessary
259 until the mean validation accuracies met the manufacturers’ recommendations. The
260 EyeLink 1000 required a mean validation accuracy limit of 0.5° , with individual points not
261 exceeding 1° (SR Research Ltd., 2010). If more than 10 calibration attempts failed, despite
262 adjustments to the EyeLink 1000, the recording session was terminated and the participant
263 was excluded from the experiment. The Pupil Labs Neon glasses are calibration-free
264 devices and were not calibrated. [However, a personal gaze offset correction was performed](#)
265 [for each participant to maximize Neon’s accuracy. This offset correction was achieved](#)
266 [directly on the companion device by fixating a single point at the center of the screen and](#)
267 [applying the correction accordingly to the procedure described on Pupil Labs website.](#)

268 **Task 1/Task 7/Task 10: Accuracy on Large and Small Grids**

269 We used fixation grids to assess the difference between the displayed target location
270 and the estimated gaze point, estimating absolute spatial accuracy and calibration
271 accuracy decay over time. [Task 10 is additionally monitoring the influence of head](#)
272 [movements on accuracy decay.](#) Two variants were employed: a large grid (7×7) and a
273 small grid (a subset of 13 points). For the grid tasks, fixation cross targets were used. For
274 the large grid, participants fixated on targets at 49 crossing points, equally spaced from
275 -7.7 to 7.7° vertically and -18.2 to 18.2° horizontally. Each target appeared once per task

276 repetition, and participants pressed the space bar after saccading to and fixating on each
277 target. The center point served as both the start and end points. We used a constrained
278 randomization procedure for the large grid to ensure uniform saccade amplitude and angle
279 distributions, maximizing the entropy of the saccade amplitude and angle histograms. The
280 small grid task was similar but involved only a subset of 13 target points that were also
281 used in the calibration procedure. The stimulus sequence was naively randomized within
282 each block for each participant.

283 **Task 2: Smooth pursuits**

284 Bullseye targets were used for the smooth pursuit task. We used Ehinger et al.
285 (2019)’s adaptation of the step-ramp smooth pursuit paradigm from Liston and Stone
286 (2014) to investigate smooth pursuits. Participants fixated on a central bullseye target and
287 pressed the space bar to start a trial, with the probe starting after a random delay sampled
288 from an exponential function (mean 500 ms). The stimuli moved along linear trajectories
289 at one of five speeds (16, 18, 20, 22, 24°/s) and trials ended when the target was 10° from
290 the center. We used 24 different orientations spanning 360°, starting each stimulus such
291 that it took 0.2 seconds to reach the center, minimizing catch-up saccades. Each smooth
292 pursuit task consisted of 20 trials, with a total of 120 trials per experiment. Each
293 participant encountered all possible combinations of speed and angle once, randomized
294 throughout the experiment. Participants were instructed to follow the target with their
295 eyes as long as possible.

296 **Task 3: Free viewing**

297 For the free viewing task, participants were presented with a total of 18 different
298 natural images, primarily patterns from Backhaus (2016). Each of the six blocks comprised
299 three randomly chosen images. The image order was randomized across the experiment,
300 and each image was shown once only. In the beginning of each trial, a fixation cross target
301 was presented at the screen center for an average of 0.9 seconds with a random jitter of 0.2
302 seconds. Afterwards, an image (900 × 720 pixels) was displayed for 6 seconds. Participants

303 were instructed to explore the images freely.

304 **Task 4: Microsaccades**

305 To elicit microsaccades, a central bullseye fixation target was displayed for 20
306 seconds, with participants instructed to maintain fixation until the target disappeared.

307 **Task 5: Blinks**

308 For the blink task, a fixation cross target was used. Participants fixated on a central
309 target and were instructed to blink each time they heard a 300 Hz sound for 100 ms. In
310 each block the sound chimed seven times with 1.5-second pauses between sounds. Each
311 sound onset was jittered by ± 0.2 seconds to reduce predictability.

312 **Task 6: Pupil Dilation**

313 For the pupil dilation task, bullseye targets were used. To stimulate pupil size
314 changes, we varied the monitor's light intensity while participants fixated on a bullseye
315 target presented in the screen center. Each block consisted of four trials with a different
316 luminance level (25%, 50%, 75%, and 100%). The order of the bright stimuli was
317 randomized within each block. At the beginning of each trial, a black screen was displayed
318 for 7 seconds (jittered by ± 0.25 seconds) to allow the pupil to reach its largest size.
319 Afterwards, one of the four target luminances was displayed for 3 seconds (jittered by
320 ± 0.25 seconds).

321 **Task 8/9: Head Movements**

322 For the head movement tasks, fixation cross targets were used. For the roll
323 movement task participants tilted their heads to align their eyes with a rotated line
324 displayed at seven different angles (-15° , -10° , -5° , 0° (horizontal), 5° , 10° , or 15° of visual
325 angle). They pressed the space bar once their eyes were in line with the target to proceed
326 to the next orientation.

327 For the yaw movement task, participants completed 15 head rotations to fixate on
328 targets positioned horizontally at five locations (-17.6° , -8.8° , 0° , 8.8° , or 17.6° of

329 [eccentricity](#)). They rotated their heads to align their noses with the target, fixated on it,
330 and pressed the space bar to confirm. The target positions were randomized within each
331 block.

332 Data analysis

333 Our data analysis follows the modular pipeline outlined by Ehinger et al. (2019),
334 from which the following subsections are adapted. Data analysis was performed using
335 Python 3 (Van Rossum & Drake, 2009), pyEDFread (Wilming et al., 2024), NumPy
336 (Harris et al., 2020), pandas (McKinney, 2010), and SciPy (Virtanen et al., 2020).
337 Visualization was done using plotnine (plotnine development team, 2024) and Matplotlib
338 (Hunter, 2007). [Experimental code, data and data analysis code are available under \[tbd\].](#)
339 [Citations, Data Transparency, Analytic Methods \(Code\), Research Materials, Design and](#)
340 [Analysis adhere to the Transparency and Openness Promotion \(TOP\) Guidelines \(Nosek](#)
341 [et al., 2015\) endorsed by the American Psychological Association. The present study did](#)
342 [not test specific hypotheses; rather, we focussed on an exploratory data analysis approach](#)
343 [to compare various gaze parameters between both eye-tracking devices. Data analysis for](#)
344 [the respective gaze parameters are described in detail below.](#)

345 Preprocessing

346 **Data Export and Transformation:** The raw EyeLink 1000 gaze data were
347 exported using the EyeLink Data Viewer software and transformed into dataframes, which
348 include calibrated gaze data mapped to the monitor coordinates. The Pupil Neon
349 eye-tracking data were automatically sent to the Pupil Labs cloud after each recording
350 session. Notably, there is no explicit calibration procedure for the Pupil Neon. In the
351 cloud, each recording is associated with the video from the scene camera and saved in a
352 workspace. After attributing the recording to a project, the data can be normalized from
353 head coordinates to world coordinates using the “Marker Mapper Enrichment” (see
354 [Coordinate System Conversion](#) section). The gaze data in normalized coordinates
355 associated with the recording time range of interest was then exported from the cloud for

356 local eye movement analysis.

357 **Coordinate System Conversion:** Since the Pupil Neon is a mobile eye-tracker
358 (head coordinate frame) and the EyeLink 1000 is a desktop eye-tracker (world coordinate
359 frame), the initial step involved converting both datasets to the same coordinate system.
360 Four QR markers were placed at the corners of the monitor to detect the display. These
361 markers were detected by the Pupil Neon scene camera and used to create a new world
362 coordinate frame. This conversion was performed directly from the Pupil Labs Cloud using
363 the “Marker Mapper Enrichment” feature. The gaze data in the world coordinate frame
364 were then exported as a dataframe, with the bottom left corner of the screen as the frame
365 origin.

366 **Gaze data synchronization:** Trigger messages were sent during the experiment
367 to mark task events. To ensure synchronized gaze information from both eye-trackers, a
368 trigger with the computer’s timestamp was sent at the beginning of the recording phase
369 before the first calibration to both devices. Gaze data from both eye-trackers were
370 synchronized by matching the recording start timestamps. If time drifts were detected
371 between recordings, synchronization was adjusted by estimating the slope difference for
372 each event trigger.

373 **Data Cleaning:** Samples marked as corrupted or where no pupil was detected
374 were excluded from further analysis, as the ones where the gaze point was outside the
375 monitor area since the experiment was performed on the screen. During this data cleaning
376 phase, *[tbd]* % of the data was removed for EyeLink 1000 (*[tbd]* samples), and *[tbd]* % for the
377 Pupil Neon (*[tbd]* samples).

378 Eye Movement Classification

379 Eye movements were defined and classified across both datasets using [an updated](#)
380 [version of Ehinger et al. \(2019\)](#) algorithmic pipeline, which applies identical algorithms to
381 both eye-trackers wherever possible. This approach ensured consistency in the comparison
382 of devices. Finally, the gaze position, eye movements, and pupil diameter associated with

each task were compared concurrently between the two eye-trackers to evaluate their performance and consistency.

Blink Classification: Blink classification differed between the two eye-trackers. The EyeLink 1000 reports blinks when the pupil is missing for several samples. [The thresholds for minimum blink duration classification can be accessed and modified.](#) In our study, blinks were defined by missing data for at least 100ms. In contrast, the Pupil Neon uses ML signal reconstruction for classification, meaning there are no missing samples (Pupil Labs blink detector, algorithm description 31.10.23). For this reason, a similar blink classification pipeline was not possible, leading us to use the proprietary algorithms. In the Pupil Neon, a machine-learning model is trained on the eye-camera video to classify eyelid opening, eyelid closing, or neither eyelid opening nor closing (see their algorithm description for more details on the parameters). After each frame is labelled, a post-processing procedure defines the eye blinks using the temporal sequence of the eyelid events. Especially, each blink is defined by onset and offset and a minimum blink duration of 100 ms. The samples associated with the 100 ms before and after a blink event were also marked as blink samples (Costela et al., 2014) and were not considered for subsequent analysis from sample data, such as saccade classification.

Saccade Classification: Saccades were classified using the velocity profile of eye movements to extract saccades, following the methods of Engbert and Kliegl (2003) and Engbert and Mergenthaler (2006). The algorithm was derived from Ehinger et al. (2019) pipeline with the hyperparameter lambda adjusted to a value of 5 for saccades classification. Unlike Ehinger et al. (2019) method, we did not interpolate the samples since the EyeLink 1000 and the Pupil Neon had constant sampling rates of 1000 Hz and 200 Hz, respectively. This classifier was applied to the sample data.

[Note: After personal communication with B. Ehinger, the saccade classification pipeline will be updated from Engbert-Mergenthaler to REMoDNaV algorithm, which still uses the velocity profile of eye movements to extract saccade.](#)

410 **Fixation Classification:** Samples not classified as blinks or saccades were labelled
411 as fixations. Fixations shorter than 50 ms were removed from the dataset. Since an
412 evaluation of the fixations classification is beyond the scope of the present study, we decided
413 to focus on the performance comparison between devices while acknowledging that the eye
414 movement classification described in this study is not optimized for mobile eye-trackers due
415 to head movements. However, we should make it clear that the tasks do not include any
416 moving objects, and the participants' heads were generally still despite no headrest
417 restrictions. Following Ehinger et al. (2019) analysis pipeline, the analysis of the gaze data
418 during the Head Movement task was only performed after the movement but not during.

419 **Smooth Pursuits classification:** An exception to this eye movements
420 classification was the Smooth Pursuit task, in which smooth pursuits were defined by gaze
421 movements with similar direction and velocity as the moving target. [Please see "Task 2:
422 Smooth pursuits" for further details.](#)

423 **Pupil Size:** The Eyelink 1000 computes the pupil size by counting the number of
424 pixels that are detected inside the pupil ellipse boundaries. Thus, the pupil size is given in
425 area. The Pupil Neon uses a deep learning algorithm (referred to as NeonNet) to compute
426 from the eye videos, and for each eye separately, a 3D model of the eyeball from which the
427 pupil sizes in diameter (mm) are extracted (Pfeffer & Dierkes, 2024). The accuracy of the
428 pupil diameter measurements is also improved by specifying the user's inter-eye distance in
429 the user's profile before the recording, which we did. The pupil diameter reported in the
430 3D eye-state measurements was converted into pupil area using $A = \frac{1}{4} \cdot \pi \cdot l_1 \cdot l_2$ where A
431 denotes the ellipsis area, l_1 denotes the semi-major axis and l_2 denotes the semi-minor axis.
432 The pupil size was then normalised to the median of a baseline period before the bright
433 stimulus onset, accounting for fluctuations due to attention or alertness.

434 Note: The 3D eye-state measurements from Pupil Labs currently give us the pupil
435 diameter D. However, we do not know yet if we can access the two ellipse axes l_1 and l_2
436 directly (ongoing communication with Pupil Labs). If we can access l_1 and l_2 , then the

437 pupil size will be converted into pupil area as described above, before being
438 baseline-normalized. If we cannot access l_1 and l_2 , then we will standardize the pupil size
439 from both eye-trackers using the z-score, and then perform the baseline normalization.

440 **Measures of Gaze Data Quality**

441 **Spatial Accuracy:** Spatial accuracy refers to the distance between the measured
442 gaze point and the target position (Holmqvist et al., 2012). It should be noted that the
443 actual gaze point might differ from the target position (e.g. due to misalignment of the
444 fovea despite the subjective direction of gaze towards the target), but we consider here the
445 target position as a proxy for the actual gaze point. This distance is often expressed by an
446 angular difference which can be computed by the cosine between the mean gaze point
447 vector and the target location vector. The vectors were converted from the Spherical
448 coordinate system to the Cartesian system to compute the cosine distance which results in
449 an angular difference between 0 and 180 degrees. The accuracy was monitored by first
450 calculating the 20% winsorized mean angular difference between the estimated gaze point
451 and the target location for each participant over blocks, and then reporting the 20%
452 winsorized mean and the interquartile range (IQR) over the already averaged values for
453 both eye-trackers. Participants may make small eye movements during fixations or
454 catch-up saccades for the ones with large amplitude, which can especially happen during
455 the calibration or the grid tasks. In such cases, multiple candidates could be considered to
456 attribute fixations' coordinates. Similarly to Ehinger et al. (2019) method, we decided to
457 select the last ongoing fixation that happened just before participants pressed the space
458 bar.

459 **Spatial Precision:** Spatial precision refers to the variability in gaze coordinate
460 estimations, reflecting the noise in the data. The less dispersed the estimations are, the
461 better the spatial precision. The measure of the spatial precision was assessed in two ways:
462 by the root mean squared (RMS) of inter-sample distances and by the standard deviation
463 (SD) of the sample locations, respectively monitoring the proximity of consecutive samples

464 and the spatial spread (see Ehinger et al. (2019) for a more detailed description). The
465 fixation spread was monitored by first calculating the 20% winsorized mean SD and RMS
466 for each participant over blocks, and then reporting the 20% winsorized mean and the
467 interquartile range (IQR) over the already averaged values for both eye-trackers.

468 **Task-specific Analyses**

469 **Task 1/Task 7/Task 10: Accuracy on Large and Small Grids.** Spatial
470 accuracy was evaluated by computing winsorized means on the offset between the displayed
471 target and the mean gaze position of the last fixation before the new target appeared, and
472 spatial precision was assessed by computing winsorized means on RMS and SD measures
473 (see Spatial Accuracy and Spatial Precision sections). The mean difference in accuracy
474 between the two eye-trackers was assessed using the 95% bootstrap confidence interval
475 (95% CI). Spatial accuracy was compared between two groups of points - the center ones
476 and the edge ones - in order to evaluate the impact of target distance-from-center on
477 eye-trackers performances. Spatial accuracy was also measured at multiple time points to
478 evaluate accuracy decay: with no decay (directly after initial calibration), after some
479 temporal drift (2/3 of the block elapsed), and after provoked head movements (yaw and
480 roll task). The decay of accuracy over time was evaluated using a robust linear mixed
481 effects model with conservative Wald's t-test p-value calculation to account for outliers.
482 Following Ehinger et al. (2019) recommendations, the model was defined by $LMM_{accuracy} \sim 1 + et \text{ session} (1 + et \text{ session} | \text{subject} \text{ block})$ and evaluated with the `robustlmm` R
483 package (Koller, 2016).

485 **Task 2: Smooth pursuits.** To analyze smooth pursuit onsets and velocities, we
486 generalized the Liston and Stone (2014) model to a Bayesian framework using STAN. The
487 x-y gaze coordinates of each trial were rotated to align with the target direction, fitting
488 data up to the first saccade exceeding 1° or up to 600 ms after trial onset. We used a
489 restricted piece-wise linear regression with a logistic transfer function for the hinge,
490 assuming normal noise. The analysis relied on classifying initial saccades accurately. Then

491 the smooth pursuit detection was monitored by first calculating the mean posterior value of
492 the hinge-point and velocity parameter for each trial, and then reporting the 20%
493 winsorized mean and the interquartile range over blocks and subjects for both eye-trackers.
494 The mean difference in smooth pursuit onsets and velocities between the two eye-trackers
495 was assessed using the 95% bootstrap confidence interval (95% CI). Additionally, we
496 recorded the number of saccades during target movement to control for sampling rate bias.

497 **Task 3: Free viewing.** The free-viewing task was analysed by first calculating the
498 20% winsorized mean fixation number, fixation durations, and saccadic amplitudes for each
499 participant over blocks, and then reporting the 20% winsorized mean and the interquartile
500 range over the already averaged values for both eye-trackers. The mean difference in
501 fixation number, fixation durations, and saccadic amplitudes between the two eye-trackers
502 was assessed using the 95% bootstrap confidence interval (95% CI). Additionally, we
503 visually compared gaze trajectories to assess the spatial inaccuracies. The first fixation on
504 the cross was excluded, and we smoothed a pixel-wise 2D histogram with a Gaussian kernel
505 ($SD = 3^\circ$) to analyze central fixation bias.

506 **Task 4: Microsaccades.** The microsaccades detection was monitored by first
507 calculating the 20% winsorized mean microsaccades number and amplitudes for each
508 participant over blocks, and then reporting the 20% winsorized mean and the interquartile
509 range over the already averaged values for both eye-trackers. The mean difference in
510 microsaccades number and amplitudes between the two eye-trackers was assessed using the
511 95% bootstrap confidence interval (95% CI). Additionally, we visually compared the main
512 sequences using the Engbert and Mergenthaler (2006) algorithm specifically for each block
513 to assess the variance of reported microsaccades.

514 **Task 5: Blinks.** The blink detection was monitored by first calculating the 20%
515 winsorized mean blink number and durations for each participant over blocks, and then
516 reporting the 20% winsorized mean and the interquartile range over the already averaged
517 values for both eye-trackers, noting the use of different blink classification algorithms (see

518 section “Eye Movement Definition and Classification”). The mean difference in blink
519 number and durations between the two eye-trackers was assessed using the 95% bootstrap
520 confidence interval (95% CI).

521 **Task 6: Pupil Dilation.** We analyzed the relative pupil areas for each luminance.
522 The normalized pupil response was calculated by dividing the pupil signal by the median
523 baseline pupil size before the bright stimulus onset. This adjustment was necessary due to
524 variations in the baseline levels, indicating potential influences such as attentional
525 processes or camera distance. The normalized pupil area is reported as a percent change
526 from the median baseline. Then the measurement of the pupil size was monitored by first
527 calculating the 20% winsorized mean normalized pupil area between 2s and 3s after
528 luminance change for each participant over blocks and luminance levels, and then reporting
529 the 20% winsorized mean and the interquartile range over the already averaged values for
530 each luminance level for both eye-trackers. The mean difference in pupil areas between the
531 two eye-trackers was assessed using the 95% bootstrap confidence interval (95% CI).

532 **Task 8/9: Head Movements.** For the roll movement task, the accuracy decay
533 was monitored by first calculating the 20% winsorized mean gaze position 0.5 seconds
534 before the button press for each participant over blocks, and then reporting the 20%
535 winsorized mean and the interquartile range over the already averaged values for both
536 eye-trackers. The gaze position was taken 0.5 seconds before the button press due to
537 continuous fixation on the center of the line during the head movement which led to no
538 new fixation detected.

539 For the yaw movement task, the accuracy decay was monitored by first calculating
540 the 20% winsorized mean gaze position at the final fixation before the participants
541 confirmed their yaw movement for each participant over blocks, and then reporting the
542 20% winsorized mean and the interquartile range over the already averaged values for both
543 eye-trackers. For both roll and yaw tasks, the mean difference in accuracy between the two
544 eye-trackers was assessed using the 95% bootstrap confidence interval (95% CI).

Acknowledgements

545

546 This project has received funding from the European Union's Horizon Europe
547 research and innovation funding program under grant agreement No 101072410 and the
548 Graduate and Professional Training Center Ulm's Early Career Incubator program.



References

- 549
- 550 Ahlström, C., Kircher, K., Nyström, M., & Wolfe, B. (2021). Eye tracking in driver
551 attention research—how gaze data interpretations influence what we learn. *Frontiers*
552 *in Neuroergonomics*, 2. <https://doi.org/10.3389/fnrgo.2021.778043>
- 553 Backhaus, D. (2016, July). *Mobiles eye-tracking: Vergleichende evaluation einer mobilen*
554 *eye-tracking brille* [Doctoral dissertation, Potsdam University].
555 <https://doi.org/10.13140/RG.2.2.35488.60165>
- 556 Baumann, C., & Dierkes, K. (2023). *Neon accuracy test report* (tech. rep.). Pupil Labs.
- 557 Beatty, J., & Lucero-Wagoner, B. (2000). The pupillary system.
- 558 Brainard, D. H., & Vision, S. (1997). The psychophysics toolbox. *Spatial vision*, 10(4),
559 433–436.
- 560 Bulling, A., & Gellersen, H. (2010). Toward mobile eye-based human-computer interaction.
561 *IEEE Pervasive Computing*, 9(4), 8–12. <https://doi.org/10.1109/MPRV.2010.86>
- 562 Cornelissen, F., Peters, E., & Palmer, J. (2002). The eyelink toolbox: Eye tracking with
563 matlab and the psychophysics toolbox. *Behavior research methods instruments &*
564 *computers*, 34(4), 613–617.
- 565 Costela, F. M., Otero-Millan, J., McCamy, M. B., Macknik, S. L., Troncoso, X. G.,
566 Jazi, A. N., Crook, S. M., & Martinez-Conde, S. (2014). Fixational Eye Movement
567 Correction of Blink-Induced Gaze Position Errors [Publisher: Public Library of
568 Science]. *PLOS ONE*, 9(10), e110889. <https://doi.org/10.1371/journal.pone.0110889>
- 569 Davis, F. D., Bagozzi, R. P., & Warshaw, P. R. (1989). User acceptance of computer
570 technology: A comparison of two theoretical models. *Management science*, 35(8),
571 982–1003.
- 572 Drewes, J., Montagnini, A., & Masson, G. S. (2011). Effects of pupil size on recorded gaze
573 position: A live comparison of two eyetracking systems. *Journal of Vision*, 11(11),
574 494. <https://doi.org/10.1167/11.11.494>
- 575 Duchowski, A. T. (2007). *Eye tracking methodology: Theory and practice*. Springer.

- 576 Duchowski, A. T. (2018). Gaze-based interaction: A 30 year retrospective. *Computers &*
577 *Graphics*, 73, 59–69. <https://doi.org/https://doi.org/10.1016/j.cag.2018.04.002>
- 578 Ehinger, B. V., Groß, K., Ibs, I., & König, P. (2019). A new comprehensive eye-tracking
579 test battery concurrently evaluating the pupil labs glasses and the eyelink 1000.
580 *PeerJ*, 7, e7086.
- 581 Einhäuser, W., Schumann, F., Bardins, S., Bartl, K., Böning, G., Schneider, E., &
582 König, P. (2007). Human eye-head co-ordination in natural exploration. *Network:*
583 *Computation in Neural Systems*, 18(3), 267–297.
584 <https://doi.org/10.1080/09548980701671094>
- 585 Engbert, R., & Kliegl, R. (2003). Microsaccades uncover the orientation of covert attention.
586 *Vision Research*, 43(9), 1035–1045.
587 [https://doi.org/https://doi.org/10.1016/S0042-6989\(03\)00084-1](https://doi.org/https://doi.org/10.1016/S0042-6989(03)00084-1)
- 588 Engbert, R., & Mergenthaler, K. (2006). Microsaccades are triggered by low retinal image
589 slip [Publisher: Proceedings of the National Academy of Sciences]. *Proceedings of the*
590 *National Academy of Sciences*, 103(18), 7192–7197.
591 <https://doi.org/10.1073/pnas.0509557103>
- 592 Funke, G., Greenlee, E., Carter, M., Dukes, A., Brown, R., & Menke, L. (2016). Which eye
593 tracker is right for your research? performance evaluation of several cost variant eye
594 trackers. *Proceedings of the Human Factors and Ergonomics Society Annual*
595 *Meeting*, 60(1), 1240–1244. <https://doi.org/10.1177/1541931213601289>
- 596 Gunawardena, N., Ginige, J. A., & Javadi, B. (2022). Eye-tracking technologies in mobile
597 devices using edge computing: A systematic review. *ACM Computing Surveys*,
598 55(8), 1–33.
- 599 Harris, C. R., Millman, K. J., van der Walt, S. J., Gommers, R., Virtanen, P.,
600 Cournapeau, D., Wieser, E., Taylor, J., Berg, S., Smith, N. J., Kern, R., Picus, M.,
601 Hoyer, S., van Kerkwijk, M. H., Brett, M., Haldane, A., del Río, J. F., Wiebe, M.,

- 602 Peterson, P., ... Oliphant, T. E. (2020). Array programming with NumPy. *Nature*,
603 585(7825), 357–362. <https://doi.org/10.1038/s41586-020-2649-2>
- 604 Henderson, J. M. (2003). Human gaze control during real-world scene perception. *Trends in*
605 *cognitive sciences*, 7(11), 498–504.
- 606 Holmqvist, K. (2017). Common predictors of accuracy, precision and data loss in 12
607 eye-trackers. *The 7th Scandinavian Workshop on Eye Tracking*.
- 608 Holmqvist, K., Andersson, R., Dewhurst, R., Jarodzka, H., & Van de Weijer, J. (2011). *Eye*
609 *tracking: A comprehensive guide to methods and measures*. Oxford University Press.
- 610 Holmqvist, K., Nyström, M., & Mulvey, F. (2012). Eye tracker data quality: What it is and
611 how to measure it. *Proceedings of the Symposium on Eye Tracking Research and*
612 *Applications*, 45–52. <https://doi.org/10.1145/2168556.2168563>
- 613 Hooge, I. T. C., Niehorster, D. C., Hessels, R. S., et al. (2023). How robust are wearable
614 eye trackers to slow and fast head and body movements? *Behavior Research*
615 *Methods*, 55, 4128–4142. <https://doi.org/10.3758/s13428-022-02010-3>
- 616 Huey, E. B. (1900). On the psychology and physiology of reading. i. *The American Journal*
617 *of Psychology*, 11(3), 283–302.
- 618 Hunter, J. D. (2007). Matplotlib: A 2d graphics environment. *Computing in Science &*
619 *Engineering*, 9(3), 90–95. <https://doi.org/10.1109/MCSE.2007.55>
- 620 Kaduk, T., Goeke, C., Finger, H., et al. (2023). Webcam eye tracking close to laboratory
621 standards: Comparing a new webcam-based system and the eyelink 1000. *Behavior*
622 *Research Methods*. <https://doi.org/10.3758/s13428-023-02237-8>
- 623 Kleiner, M., Brainard, D., & Pelli, D. (2007). What's new in psychtoolbox-3? *Perception*.
- 624 Koller, M. (2016). Robustlmm: An r package for robust estimation of linear mixed-effects
625 models. *Journal of Statistical Software*, 75(6), 1–24.
626 <https://doi.org/10.18637/jss.v075.i06>
- 627 Krauzlis, R. J. (2004). Recasting the smooth pursuit eye movement system. *Journal of*
628 *neurophysiology*, 91(2), 591–603.

- 629 Liston, D. B., & Stone, L. S. (2014). Oculometric assessment of dynamic visual processing.
630 *Journal of Vision*, 14(14), 12–12. <https://doi.org/10.1167/14.14.12>
- 631 MacInnes, J. J., Iqbal, S., Pearson, J., & Johnson, E. N. (2018). Wearable eye-tracking for
632 research: Automated dynamic gaze mapping and accuracy/precision comparisons
633 across devices. *bioRxiv*, 299925.
- 634 Majaranta, P., & Bulling, A. (2014). Eye tracking and eye-based human–computer
635 interaction. In S. Fairclough & K. Gilleade (Eds.), *Advances in physiological*
636 *computing*. Springer. https://doi.org/10.1007/978-1-4471-6392-3_3
- 637 Mancini, M., Cherubino, P., Cartocci, G., Martinez, A., Di Flumeri, G., Petruzzellis, L.,
638 Cimini, M., Aricò, P., Trettel, A., & Babiloni, F. (2022). Esports and visual
639 attention: Evaluating in-game advertising through eye-tracking during the game
640 viewing experience. *Brain Sciences*, 12(10).
641 <https://doi.org/10.3390/brainsci12101345>
- 642 Martinez-Conde, S., Macknik, S., & Hubel, D. (2004). The role of fixational eye movements
643 in visual perception. *Nature Reviews Neuroscience*, 5, 229–240.
644 <https://doi.org/10.1038/nrn1348>
- 645 Martinez-Conde, S., Otero-Millan, J., & Macknik, S. L. (2013). The impact of
646 microsaccades on vision: Towards a unified theory of saccadic function. *Nature*
647 *Reviews Neuroscience*, 14(2), 83–96.
- 648 Mathôt, S., & Vilotijević, A. (2023). Methods in cognitive pupillometry: Design,
649 preprocessing, and statistical analysis. *Behavior Research Methods*, 55(6),
650 3055–3077. <https://doi.org/10.3758/s13428-022-01957-7>
- 651 MATLAB. (2016). *R2016b*. The MathWorks Inc.
- 652 MATLAB. (2021). *R2021a*. The MathWorks Inc.
- 653 McKinney, W. (2010). Data Structures for Statistical Computing in Python. In
654 S. van der Walt & J. Millman (Eds.), *Proceedings of the 9th Python in Science*
655 *Conference* (pp. 56–61). <https://doi.org/10.25080/Majora-92bf1922-00a>

- 656 Niehorster, D. C., Santini, T., Hessels, R. S., et al. (2020). The impact of slippage on the
657 data quality of head-worn eye trackers. *Behavior Research Methods*, *52*, 1140–1160.
658 <https://doi.org/10.3758/s13428-019-01307-0>
- 659 Nosek, B. A., Alter, G., Banks, G. C., Borsboom, D., Bowman, S. D., Breckler, S. J.,
660 Buck, S., Chambers, C. D., Chin, G., Christensen, G., Contestabile, M., Dafoe, A.,
661 Eich, E., Freese, J., Glennerster, R., Goroff, D., Green, D. P., Hesse, B.,
662 Humphreys, M., . . . Yarkoni, T. (2015). Promoting an open research culture.
663 *Science*, *348*(6242), 1422–1425. <https://doi.org/10.1126/science.aab2374>
- 664 Pelli, D. G. (1997). The videotoolbox software for visual psychophysics: Transforming
665 numbers into movies. *Spatial vision*, *10*(4), 437–442.
- 666 Pentus, K., Ploom, K., Mehine, T., Koiv, M., Tempel, A., & Kuusik, A. (2020). Mobile and
667 stationary eye tracking comparison—package design and in-store results. *Journal of*
668 *Consumer Marketing*, *37*(3), 259–269.
- 669 Pfeffer, T., & Dierkes, K. (2024). *Neon pupillometry test report* (tech. rep.). Pupil Labs.
670 <https://doi.org/10.5281/zenodo.10057185>
- 671 plotnine development team, T. (2024). Plotnine: A grammar of graphics for python.
672 <https://doi.org/https://doi.org/10.5281/zenodo.1325308>
- 673 Rayner, K. (2009). The 35th sir frederick bartlett lecture: Eye movements and attention in
674 reading, scene perception, and visual search. *Quarterly Journal of Experimental*
675 *Psychology*, *62*(8), 1457–1506.
- 676 Rayner, K. (1998). Eye movements in reading and information processing: 20 years of
677 research. *Psychological bulletin*, *124*(3), 372.
- 678 Rolfs, M. (2009). Microsaccades: Small steps on a long way. *Vision Research*, *49*(20),
679 2415–2441. <https://doi.org/10.1016/j.visres.2009.08.010>
- 680 Schleicher, R., Galley, N., Briest, S., & Galley, L. (2008). Blinks and saccades as indicators
681 of fatigue in sleepiness warnings: Looking tired? *Ergonomics*, *51*(7), 982–1010.
682 <https://doi.org/10.1080/00140130701817062>

- 683 SR Research Ltd. (2022). *Eyelink data viewer*.
- 684 SR Research Ltd., S. (2010). Eyelink 1000 user manual.
685 <https://www.sr-research.com/support-options/learning-resources/>
- 686 Takahashi, R., Suzuki, H., Chew, J. Y., Ohtake, Y., Nagai, Y., & Ohtomi, K. (2018). A
687 system for three-dimensional gaze fixation analysis using eye tracking glasses.
688 *Journal of Computational Design and Engineering*, 5(4), 449–457.
689 <https://doi.org/10.1016/j.jcde.2017.12.007>
- 690 Thaler, L., Schütz, A., Goodale, M., & Gegenfurtner, K. (2013). What is the best fixation
691 target? the effect of target shape on stability of fixational eye movements. *Vision*
692 *Research*, 76, 31–42. <https://doi.org/https://doi.org/10.1016/j.visres.2012.10.012>
- 693 Titz, J., Scholz, A., & Sedlmeier, P. (2018). Comparing eye trackers by correlating their
694 eye-metric data. *Behavior research methods*, 50(5), 1853–1863.
695 <https://doi.org/10.3758/s13428-017-0954-y>
- 696 Van Rossum, G., & Drake, F. L. (2009). *Python 3 reference manual*. CreateSpace.
- 697 Virtanen, P., Gommers, R., Oliphant, T. E., Haberland, M., Reddy, T., Cournapeau, D.,
698 Burovski, E., Peterson, P., Weckesser, W., Bright, J., van der Walt, S. J., Brett, M.,
699 Wilson, J., Millman, K. J., Mayorov, N., Nelson, A. R. J., Jones, E., Kern, R.,
700 Larson, E., . . . SciPy 1.0 Contributors. (2020). SciPy 1.0: Fundamental Algorithms
701 for Scientific Computing in Python. *Nature Methods*, 17, 261–272.
702 <https://doi.org/10.1038/s41592-019-0686-2>
- 703 Wang, D., Mulvey, F. B., Pelz, J. B., et al. (2017). A study of artificial eyes for the
704 measurement of precision in eye-trackers. *Behavior Research Methods*, 49, 947–959.
705 <https://doi.org/10.3758/s13428-016-0755-8>
- 706 Wilming, N., Morton, N., & Ehinger, B. (2024). Github repository of pyedfread.
707 <https://github.com/s-ccs/pyedfread/tree/master>
- 708 Zeromq. (2024).

Question	Hypothesis	Sampling plan	Analysis Plan	Rationale for deciding the sensitivity of the test for confirming or disconfirming the hypothesis	Interpretation given different outcomes	Theory that could be shown wrong by the outcomes
How accurate and precise are the Pupil Neon recordings when compared to the Eyelink 1000?	-	For logistical lab reasons, participants will be recruited in a time window of 2 weeks. We take however many we can get within that time with a minimum of 25 participants (cf. Ehinger, 2019).		-	-	Eyelink 1000 is the gold standard for eye-tracking measurements.
Accuracy tasks (large & small grid task)	-		Spatial accuracy is evaluated by computing the 20% winsorized mean (WS) offset between the displayed target and the mean gaze position of the last fixation before the new target appeared and its interquartile range (IQR), and spatial precision was assessed by computing WS on RMS of inter-sample distances and SD measures of sample locations and its IQR. The mean difference between the eye-trackers is assessed using the 95% bootstrap confidence interval (95% CI). The decay of accuracy over time was evaluated using a robust linear mixed effects model with conservative Wald's t-test p-value calculation to account for outliers.	-	The more significant is the LMM, the stronger is the decay of accuracy over time. Determine if Neon accuracy and precision can be comparable to Eyelink 1000.	
Smooth pursuit task	-		First calculating the mean posterior value of the hinge-point and velocity parameter for each trial, and then reporting the 20% WS and the IQR over blocks and subjects. The mean difference between the eye-trackers is assessed using the 95% CI. Number of saccades recorded during target movement to control for sampling rate bias.	-	Determine if Neon smooth pursuit detection can be comparable to Eyelink 1000.	

Free viewing task	-		First calculating the 20% WS mean fixation number, fixation durations, and saccadic amplitudes for each participant, and then reporting the 20% WS and the IQR over the averaged values. The mean difference between the eye-trackers is assessed using the 95% CI. Visual comparison of gaze trajectories to assess the spatial inaccuracies.	-	Determine if Neon fixation and saccade detection can be comparable to Eyelink 1000.
Microsaccade task	-		First calculating the 20% WS microsaccades number and amplitudes for each participant, and then reporting the 20% WS and the IQR over the averaged values. The mean difference between the eye-trackers is assessed using the 95% CI. Visual comparison of the main sequences using the Engbert (2006) algorithm to assess the variance of reported microsaccades.	-	Determine if Neon microsaccade detection can be comparable to Eyelink 1000.
Blinks task	-		First calculating the 20% WS blink number and durations for each participant, and then reporting the 20% WS and the IQR over the averaged values. The mean difference between the eye-trackers is assessed using the 95% CI.	-	Determine if Neon blink detection can be comparable to Eyelink 1000.
Pupil dilation task	-		First calculating the 20% WS pupil area between 2s and 3s after luminance change for each participant, and then reporting the 20% WS and the IQR over the averaged values for each luminance level. The mean difference between the eye-trackers is assessed using the 95% CI.	-	Determine if Neon measurement of the pupil size can be comparable to Eyelink 1000.

Head rolls task	-		First calculating the 20% WS gaze position 0.5 seconds before the button press for each participant, and then reporting the 20% WS and the IQR over the averaged values. The mean difference between the eye-trackers is assessed using the 95% CI.	-	Determine if Neon accuracy after roll movements can be comparable to Eyelink 1000.	
Head yaws task	-		First calculating the 20% WS gaze position at the final fixation before the participants confirmed their yaw movement for each participant, and then reporting the 20% WS and the IQR over the averaged values. The mean difference between the eye-trackers is assessed using the 95% CI.	-	Determine if Neon accuracy after yaw movements can be comparable to Eyelink 1000.	

Guidance Notes

- **Question:** articulate each research question being addressed in one sentence.
- **Hypothesis:** where applicable, a prediction arising from the research question, stated in terms of specific variables rather than concepts. Where the testability of one or more hypotheses depends on the verification of auxiliary assumptions (such as positive controls, tests of intervention fidelity, manipulation checks, or any other quality checks), any tests of such assumptions should be listed as hypotheses. Stage 1 proposals that do not seek to test hypotheses can ignore or delete this column.
- **Sampling plan:** For proposals using inferential statistics, the details of the statistical sampling plan for the specific hypothesis (e.g power analysis, Bayes Factor Design Analysis, ROPE etc). For proposals that do not use inferential statistics, include a description and justification of the sample size.
- **Analysis plan:** For hypothesis-driven studies, the specific test(s) that will confirm or disconfirm the hypothesis. For non-hypothesis-driven studies, the test(s) that will answer the research question.
- **Rationale for deciding the sensitivity of the test for confirming or disconfirming the hypothesis:** For hypothesis-driven studies that employ inferential statistics, an explanation of how the authors determined a relevant effect size for statistical power analysis, equivalence testing, Bayes factors, or other approach.
- **Interpretation given different outcomes:** A prospective interpretation of different potential outcomes, making clear which outcomes would confirm or disconfirm the hypothesis.
- **Theory that could be shown wrong by the outcomes:** Where the proposal is testing a theory, make clear what theory could be shown to be wrong, incomplete, or otherwise inadequate by the outcomes of the research.